Is 9D localization possible with unsynchronized LEO Satellites?

Don-Roberts Emenonye, Harpreet S. Dhillon, and R. Michael Buehrer

***Abstract*—In this paper, we ask if 9D localization (3D position, 3D velocity, and 3D orientation estimation) is possible with the signals received from low earth orbit (LEO) satellites. To answer this question, we define a system model that captures i) the possibility of a time offset between LEOs caused by having cheap synchronization clocks, ii) the possibility of a frequency offset between LEOs, and iii) multiple transmission time slots from a particular LEO. We transform the Fisher information matrix (FIM) for the channel parameters to the FIM for the location parameters and show the possible localization conditions. Subsequently, we derive the FIM for the 9D localization (3D position, 3D orientation, and 3D velocity estimation) in terms of the FIM for the 3D localization. With these derivations, we show that even in the presence of time and frequency offsets between the LEOs, it is possible to perform 9D localization (3D position, 3D velocity, and 3D orientation estimation) of a receiver by utilizing the signals from three LEO satellites observed during three transmission time slots received through multiple receive antennas.**

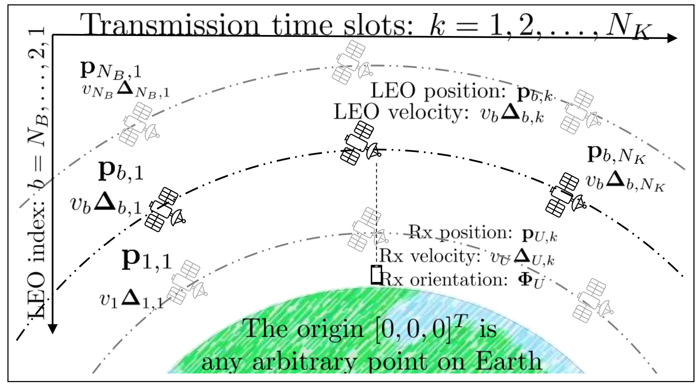

Figure 1. LEO-based localization systems with N_B LEOs transmitting during N_K transmission time slots to a receiver with N_U antennas.

I. Introduction

There has been renewed interest in the use of low earth orbit satellites as evidenced by the launch of several new satellites into existing LEO constellations, such as Orbcomm, Iridium, and Globalstar, as well as the creation of new constellations such as Boeing, SpaceMobile, Onevveb, Telesat, Kuiper, and Starlink [1]. Because this cluster of mega-constellations will be closer to the earth than the current satellites in global navigation satellite systems (GNSS), they will have shorter propagation delays and encounter lower losses, thereby providing greater potential accuracy in specific localization scenarios. Moreover, LEO satellites could be used when the GNSS signals are unavailable (such as in deep urban canyons, under dense foliage, during unintentional interference, and intentional jamming) or untrustworthy (e.g., under malicious spoofing attacks). Due to these reasons, utilizing these LEO satellites for localization is an increasing research direction.

A. Prior art

The authors in [2] provide an opportunistic experimental framework to use at least eight Doppler shift measurements to give estimates for the 3D position, 3D velocity, time offset, and time offset rate. In [3], an opportunistic framework that combines inertial measurement units with the signals from the LEO satellites is developed to experimentally estimate the position of LEO satellites, the time offset, and the LEO orbit. Authors in [4] demonstrate experimentally that the signals from two Orbcomm satellites can be used to opportunistically track an unmanned aerial vehicle (UAV) for two minutes with a position error of 15 m. In [5], an opportunistic framework using Doppler measurement taken from Orbocomm satellites over multiple time intervals is used to estimate the orbital parameters and receiver position. Authors in [6] develop an opportunistic framework to detect reference signals from six Starlink satellites, and subsequently use this framework to achieve a receiver positioning error of 20 m. The authors in [7] propose an opportunistic framework to combine IMU measurements with range and Doppler measurements. This framework utilizes two Orbcomm, one Iridium and three Starlink satellites to achieve position errors of 27.1 m and 18.4 m, respectively. A ground receiver localizes itself while estimating the noise covariance matrix of a single Orbcomm satellite with Doppler observed over time in [8].

In summary, current research has yet to provide a rigorous explanation of the available information in LEO satellites from the same or different constellations that are received by a multiple antenna receiver during multiple transmission time slots. Hence, in this paper, with the assumption that the LEO orbits are known, we use information theory to rigorously characterize this available information and its utility for the 9D localization of a receiver (3D position, 3D orientation, and 3D velocity estimation) even in the presence of time and frequency offsets between the LEOs.

D.-R. Emenonye, H. S. Dhillon, and R. M. Buehrer are with Wireless@VT, Bradley Department of Electrical and Computer Engineering, Virginia Tech, Blacksburg, VA, 24061, USA. Email: {donroberts, hdhillon, rbuehrer}@vt.edu. The support of the US National Science Foundation (Grants ECCS-2030215, CNS-1923807, and CNS-2107276) is gratefully acknowledged.

II. System Model

We consider N_B single antenna LEO satellites, each communicating with a receiver with N_U antennas, through transmissions in N_K different time slots. The transmission slots are spaced by Δ_t. At the k^{th} transmission time slot, the N_B LEO satellites are located at $\boldsymbol{p}_{b,k}, \quad b \in \{1, 2, \cdots, N_B\}$ and $k \in \{1, 2, \cdots, N_K\}$. The points, $\boldsymbol{p}_{b,k}$, are described with respect to a global origin. During the k^{th} time slot, the receiver has an arbitrary but known geometry with its centroid located at $\boldsymbol{p}_{U,k}$. During the k^{th} time slot, the point, $\boldsymbol{s}_u$, describes the u^{th} receive antenna with respect to the centroid while the point, $\boldsymbol{p}_{u,k}$, describes the position of this element with respect to the global origin as $\boldsymbol{p}_{u,k} = \boldsymbol{p}_{U,k} + \boldsymbol{s}_u$. The point, $\boldsymbol{s}_u$, can be written as $\boldsymbol{s}_u = \boldsymbol{Q}_U \tilde{\boldsymbol{s}}_u$ where $\tilde{\boldsymbol{s}}_u$ aligns with the global reference axis and $\boldsymbol{Q}_U = \boldsymbol{Q}(\alpha_U, \psi_U, \varphi_U)$ defines a 3D rotation matrix [9]. The orientation angles of the receiver are vectorized as $\boldsymbol{\Phi}_U = [\alpha_U, \psi_U, \varphi_U]^{\mathrm{T}}$. The centroid of the receiver at point, $\boldsymbol{p}_{U,k}$ with respect to the b^{th} LEO can be written as $\boldsymbol{p}_{U,k} = \boldsymbol{p}_{b,k} + d_{bU,k}\boldsymbol{\Delta}_{bU,k}$ where $d_{bU,k}$ is the distance from point $\boldsymbol{p}_{b,k}$ to point $\boldsymbol{p}_{U,k}$ and $\boldsymbol{\Delta}_{bU,k}$ is the corresponding unit direction vector $\boldsymbol{\Delta}_{bU,k} = [\cos\phi_{bU,k}\sin\theta_{bU,k}, \sin\phi_{bU,k}\sin\theta_{bU,k}, \cos\theta_{bU,k}]^{\mathrm{T}}$. During the k^{th} transmission time slot, the angles $\phi_{bU,k}$ and $\theta_{bU,k}$ represent the angle in the azimuth and elevation from the b^{th} LEO satellite to the receiver.

A. Transmit and Receive Processing

The N_B LEO satellites transmit in N_K different time slots, each of equal durations. At time t, during the k^{th} time slot, the b^{th} LEO satellite uses quadrature modulation and transmits the following signal to the receiver $x_{b,k}[t] = s_{b,k}[t]\exp(j2\pi f_c t)$, where $s_{b,k}[t]$ is the complex signal envelope of the signal transmitted by the b^{th} LEO satellite during the k^{th} time slot, and $f_c = c/\lambda$ is the operating frequency of LEO satellites. The speed of light is c, and λ is the operating wavelength. The channel model from the LEO satellites to the receiver consists only of the LOS paths. With this channel model and the transmit signal, the signal at the u^{th} receive antenna during the k^{th} time slot is

$$\begin{aligned} y_{u,k}[t] &= \sum_{b}^{N_B} y_{bu,k}[t], \\ &= \sum_{b=1}^{N_b} \beta_{bu,k}\sqrt{2}\Re\left\{s_{b,k}[t_{obu,k}]\exp(j(2\pi f_{ob,k} t_{obu,k}))\right\} \\ &+ n_{u,k}[t], \\ &= \mu_{u,k}[t] + n_{u,k}[t], \end{aligned} \tag{1}$$

where $\mu_{u,k}[t]$ and $n_{u,k}[t] \sim \mathcal{CN}(0, N_0)$ are the noise-free part (useful part) of the signal and the Fourier transformed thermal noise local to the receiver's antenna array, respectively. Also, $\beta_{bu,k}$ is the channel gain from the b^{th} LEO satellite observed at the u^{th} receive antenna during the k^{th} time slot, $f_{ob,k} = f_c(1 - \nu_{b,k}) + \epsilon_b$ is the observed frequency at receiver with respect to the b^{th} LEO satellite, and $t_{obu,k} = t - \tau_{bu,k} + \delta_b$ is the effective time duration. In the observed frequency, $\nu_{b,k}$ is the Doppler with respect to the b^{th} LEO satellite, and ϵ_b is the frequency offset measured with respect to the b^{th} LEO satellite.

In the effective time duration, δ_b is the time offset at the receiver measured with respect to the b^{th} LEO satellite, and the delay from the u^{th} receive antenna to the b^{th} LEO satellite during the k^{th} time slot is

$$\tau_{bu,k} \triangleq \frac{\|\mathbf{p}_{u,k} - \mathbf{p}_{b,k}\|}{c}.$$

Here, the position of the b^{th} LEO satellite and the u^{th} receive antenna during the k^{th} time slot is $\mathbf{p}_{b,k} = \mathbf{p}_{b,o} + \tilde{\mathbf{p}}_{b,k}$, and $\mathbf{p}_{u,k} = \mathbf{p}_{u,o} + \tilde{\mathbf{p}}_{U,k}$, respectively. Here, $\mathbf{p}_{b,o}$ and $\mathbf{p}_{u,o}$ are the reference points of the b^{th} LEO satellite and the u^{th} receive antenna, respectively. The distance travelled by the b^{th} LEO satellite and the u^{th} receive antenna are $\tilde{\mathbf{p}}_{b,k}$ and $\tilde{\mathbf{p}}_{u,k}$, respectively. These traveled distances can be described as $\tilde{\mathbf{p}}_{b,k} = (k-1)\Delta_t v_b \boldsymbol{\Delta}_{b,k}$, and $\tilde{\mathbf{p}}_{U,k} = (k-1)\Delta_t v_U \boldsymbol{\Delta}_{U,k}$, respectively. Here, v_b and v_U are speeds of the b^{th} LEO satellite and receiver, respectively. The associated directions are defined as $\boldsymbol{\Delta}_{b,k} = [\cos\phi_{b,k}\sin\theta_{b,k}, \sin\phi_{b,k}\sin\theta_{b,k}, \cos\theta_{b,k}]^{\mathrm{T}}$ and $\boldsymbol{\Delta}_{U,k} = [\cos\phi_{U,k}\sin\theta_{U,k}, \sin\phi_{U,k}\sin\theta_{U,k}, \cos\theta_{U,k}]^{\mathrm{T}}$, respectively. Now, the velocity of the b^{th} LEO satellite and the velocity of the receiver are $\boldsymbol{v}_{b,k} = v_b\boldsymbol{\Delta}_{b,k}$ and $\boldsymbol{v}_{U,k} = v_U\boldsymbol{\Delta}_{U,k}$, respectively. Hence, the Doppler observed by the receiver from the b^{th} LEO satellite is $\nu_{b,k} = \boldsymbol{\Delta}_{bU,k}^{\mathrm{T}} \frac{(\boldsymbol{v}_{b,k} - \boldsymbol{v}_{U,k})}{c}$.

B. Properties of the Received Signal

In this section, we discuss the properties that are observable in the signal at the receiver across all receive antennas and during all the transmission slots. To accomplish this, we consider the Fourier transform of the baseband signal that is transmitted by the b^{th} LEO satellite at time t during the k^{th} time slot $S_{b,k}[f] \triangleq \frac{1}{\sqrt{2\pi}}\int_{-\infty}^{\infty} s_{b,k}[t]\exp(-j2\pi f t) \quad dt$. This Fourier transform is called the spectral density.

1) Effective Baseband Bandwidth: This can be viewed as the average of the squared of all frequencies normalized by the area occupied by the spectral density, $S_{b,k}$. Mathematically, the effective baseband bandwidth is $\alpha_{1b,k} \triangleq \left(\frac{\int_{-\infty}^{\infty} f^2 |S_{b,k}[f]|^2 df}{\int_{-\infty}^{\infty} |S_{b,k}[f]|^2 df}\right)^{\frac{1}{2}}$.

2) Baseband-Carrier Correlation (BCC): Mathematically, the BCC is $\alpha_{2b,k} \triangleq \frac{\int_{-\infty}^{\infty} f |S_{b,k}[f]|^2 df}{\left(\int_{-\infty}^{\infty} f^2 |S_{b,k}[f]|^2 df\right)^{\frac{1}{2}} \left(\int_{-\infty}^{\infty} |S_{b,k}[f]|^2 df\right)^{\frac{1}{2}}}$. In later sections, the term $\alpha_{2b,k}$ will help provide a compact representation of the mathematical description of the available information in the received signals.

3) Received Signal-to-Noise Ratio: The SNR is the ratio of the power of the signal across its occupied frequencies to the noise spectral density. Mathematically, the SNR is $\underset{bu,k}{\mathrm{SNR}} \triangleq \frac{8\pi^2|\beta_{bu,k}|^2}{N_0}\int_{-\infty}^{\infty} |S_{b,k}[f]|^2 df$.

The mathematical description of the available information useful for localization is written in terms of these received signal properties.

III. Available Information in the Received Signal

In this section, we define the parameters, both geometric channel parameters and nuisance parameters. The definition of these parameters serves as an intermediate step to investigating the available geometric information provided by LEOs, which subsequently helps the investigation of the feasibility of LEO-based localization under different types of LEO constellations, number of LEOs, beam split, and number of receive antennas.

A. Error Bounds on Parameters

The analysis in this section is based on the received signal given by (1), which is obtained from N_B LEO satellites on N_U receive antennas during N_K distinct time slots of T durations each. The parameters observable in the signal received by a receiver from the b^{th} LEO satellite on its N_U receive antenna during the N_K different time slots are subsequently presented. The delays observed across the N_U receive antennas during the k^{th} time slots are presented in vector form $\boldsymbol{\tau}_{b,k} \triangleq \left[\tau_{b1,k}, \tau_{b2,k}, \cdots, \tau_{bN_U,k}\right]^{\mathrm{T}}$, then the delays across the N_U receive antennas during all N_K time slots are also vectorized as follows $\boldsymbol{\tau}_b \triangleq \left[\boldsymbol{\tau}_{b,1}^{\mathrm{T}}, \boldsymbol{\tau}_{b,2}^{\mathrm{T}}, \cdots, \boldsymbol{\tau}_{b,N_K}^{\mathrm{T}}\right]^{\mathrm{T}}$.The Doppler observed with respect to the b^{th} LEO satellite across all the N_K transmission time slots is $\boldsymbol{\nu}_b \triangleq \left[\nu_{b,1}, \nu_{b,2}, \cdots, \nu_{b,N_K}\right]^{\mathrm{T}}$. Next, the channel gain across the N_U receive antennas during the k^{th} time slots are presented in vector form $\boldsymbol{\beta}_{b,k} \triangleq \left[\beta_{b1,k}, \beta_{b2,k}, \cdots, \beta_{bN_U,k}\right]^{\mathrm{T}}$, then the delays across the N_U receive antennas during all N_K time slots are also vectorized as follows $\boldsymbol{\beta}_b \triangleq \left[\boldsymbol{\beta}_{b,1}^{\mathrm{T}}, \boldsymbol{\beta}_{b,2}^{\mathrm{T}}, \cdots, \boldsymbol{\beta}_{b,N_K}^{\mathrm{T}}\right]^{\mathrm{T}}$. Note that if there is no beam split, the channel gain remains constant across all antennas and is simply $\boldsymbol{\beta}_b \triangleq \left[\beta_{b,1}, \beta_{b,2}, \cdots, \beta_{b,N_K}\right]^{\mathrm{T}}$. Moreover, if the channel gain is constant across all time slots, we can further represent the b^{th} LEO transmission by the scalar, β_b. Finally, with these vectorized forms, the total parameters observable in the signals received at a receiver from the b^{th} LEO satellite on its N_U receive antenna during the N_K different time slots are vectorized as follows $\boldsymbol{\eta}_b^{\mathrm{T}} \triangleq \left[\boldsymbol{\tau}_b^{\mathrm{T}}, \boldsymbol{\nu}_b^{\mathrm{T}}, \boldsymbol{\beta}_b^{\mathrm{T}}, \delta_b, \epsilon_b\right]^{\mathrm{T}}$. All signals observable from all N_B LEO satellites across N_U receive antennas during the N_K different time slots are vectorized as $\boldsymbol{\eta}^{\mathrm{T}} \triangleq \left[\boldsymbol{\eta}_1^{\mathrm{T}}, \boldsymbol{\eta}_2^{\mathrm{T}}, \cdots, \boldsymbol{\eta}_{N_B}^{\mathrm{T}}\right]^{\mathrm{T}}$. After specifying the parameters that are present in the signals received from the LEO satellites - considering the time slots and receive antennas, we present the mathematical preliminaries needed for further discussions.

B. Mathematical Preliminaries

Although we have specified the parameters in the signals received in a LEO-based localization system, we still have to investigate the estimation accuracy achievable when estimating these parameters. Moreover, it's unclear whether all the parameters presented are separately observable and can contribute to a localization framework. One way of answering these two questions is by using the FIM.

Definition 1. *The general FIM for a parameter vector, $\boldsymbol{\eta}$, defined as $\mathbf{J}_{\boldsymbol{y};\boldsymbol{\eta}} = \boldsymbol{F}_{\boldsymbol{y};\boldsymbol{\eta}}(\boldsymbol{y};\boldsymbol{\eta};\boldsymbol{\eta},\boldsymbol{\eta})$ is the summation of the FIM obtained from the likelihood due to the observations defined as $\mathbf{J}_{\boldsymbol{y}|\boldsymbol{\eta}} = \boldsymbol{F}_{\boldsymbol{y}}(\boldsymbol{y}|\boldsymbol{\eta};\boldsymbol{\eta},\boldsymbol{\eta})$ and the FIM from* a priori *information about the parameter vector defined as $\mathbf{J}_{\boldsymbol{\eta}} = \boldsymbol{F}_{\boldsymbol{\eta}}(\boldsymbol{\eta};\boldsymbol{\eta},\boldsymbol{\eta})$. In mathematical terms, we have*

$$\begin{aligned}\mathbf{J}_{\boldsymbol{y};\boldsymbol{\eta}} &\triangleq -\mathbb{E}_{\boldsymbol{y};\boldsymbol{\eta}}\left[\frac{\partial^2 \ln \chi(\boldsymbol{y};\boldsymbol{\eta})}{\partial \boldsymbol{\eta} \partial \boldsymbol{\eta}^{\mathrm{T}}}\right] \\ &= -\mathbb{E}_{\boldsymbol{y}}\left[\frac{\partial^2 \ln \chi(\boldsymbol{y}|\boldsymbol{\eta})}{\partial \boldsymbol{\eta} \partial \boldsymbol{\eta}^{\mathrm{T}}}\right] - \mathbb{E}_{\boldsymbol{\eta}}\left[\frac{\partial^2 \ln \chi(\boldsymbol{\eta})}{\partial \boldsymbol{\eta} \partial \boldsymbol{\eta}^{\mathrm{T}}}\right] \\ &= \mathbf{J}_{\boldsymbol{y}|\boldsymbol{\eta}} + \mathbf{J}_{\boldsymbol{\eta}},\end{aligned} \tag{2}$$

where $\chi(\boldsymbol{y};\boldsymbol{\eta})$ denotes the probability density function (PDF) of $\boldsymbol{y}$ and $\boldsymbol{\eta}$.

Definition 2. *Given a parameter vector, $\boldsymbol{\eta} \triangleq \left[\boldsymbol{\eta}_1^{\mathrm{T}}, \boldsymbol{\eta}_2^{\mathrm{T}}\right]^{\mathrm{T}}$, where $\boldsymbol{\eta}_1$ is the parameter of interest, the resultant FIM has the structure*

$$\mathbf{J}_{\boldsymbol{y};\boldsymbol{\eta}} = \begin{bmatrix} \mathbf{J}_{\boldsymbol{y};\boldsymbol{\eta}_1} & \mathbf{J}_{\boldsymbol{y};\boldsymbol{\eta}_1,\boldsymbol{\eta}_2} \\ \mathbf{J}_{\boldsymbol{y};\boldsymbol{\eta}_1,\boldsymbol{\eta}_2}^{\mathrm{T}} & \mathbf{J}_{\boldsymbol{y};\boldsymbol{\eta}_2} \end{bmatrix},$$

where $\boldsymbol{\eta} \in \mathbb{R}^N, \boldsymbol{\eta}_1 \in \mathbb{R}^n, \mathbf{J}_{\boldsymbol{y};\boldsymbol{\eta}_1} \in \mathbb{R}^{n\times n}, \mathbf{J}_{\boldsymbol{y};\boldsymbol{\eta}_1,\boldsymbol{\eta}_2} \in \mathbb{R}^{n\times(N-n)}$, and $\mathbf{J}_{\boldsymbol{y};\boldsymbol{\eta}_2} \in \mathbb{R}^{(N-n)\times(N-n)}$ with $n < N$, and the EFIM [10] of parameter $\boldsymbol{\eta}_1$ is given by $\mathbf{J}_{\boldsymbol{y};\boldsymbol{\eta}_1}^{\mathrm{e}} = \mathbf{J}_{\boldsymbol{y};\boldsymbol{\eta}_1} - \mathbf{J}_{\boldsymbol{y};\boldsymbol{\eta}_1}^{nu} = \mathbf{J}_{\boldsymbol{y};\boldsymbol{\eta}_1} - \mathbf{J}_{\boldsymbol{y};\boldsymbol{\eta}_1,\boldsymbol{\eta}_2}\mathbf{J}_{\boldsymbol{y};\boldsymbol{\eta}_2}^{-1}\mathbf{J}_{\boldsymbol{y};\boldsymbol{\eta}_1,\boldsymbol{\eta}_2}^{\mathrm{T}}$.

C. Fisher Information Matrix for Channel Parameters

In the definitions of the FIM and EFIM given in the previous section, the expression of the likelihood of the received signal conditioned on the parameter vector is required. This likelihood for the received signal conditioned on the parameter vector is defined considering the N_B LEO satellites, N_U receive antennas, and the N_K time slots, and is presented in [1]. Subsequently, this FIM due to the observations from the N_B LEO satellite, received across the N_U antennas, and during the N_K distinct time slots can be computed with the likelihood function and Definition 1, and it results in the diagonal matrix[1]. $\mathbf{J}_{\boldsymbol{y}|\boldsymbol{\eta}} = \boldsymbol{F}_{\boldsymbol{y}}(\boldsymbol{y}|\boldsymbol{\eta};\boldsymbol{\eta},\boldsymbol{\eta}) = \operatorname{diag}\left\{\boldsymbol{F}_{\boldsymbol{y}}(\boldsymbol{y}|\boldsymbol{\eta};\boldsymbol{\eta}_1,\boldsymbol{\eta}_1), \ldots, \boldsymbol{F}_{\boldsymbol{y}}(\boldsymbol{y}|\boldsymbol{\eta};\boldsymbol{\eta}_{N_B},\boldsymbol{\eta}_{N_B})\right\}$. The entries in FIM due to the observations of the received signals from b^{th} LEO satellite can be obtained through the simplified expression. $\boldsymbol{F}_{\boldsymbol{y}}(\boldsymbol{y}|\boldsymbol{\eta};\boldsymbol{\eta}_b,\boldsymbol{\eta}_b) = \frac{1}{N_0}\sum_{u,k}^{N_U N_K} \Re\left\{\int \nabla_{\boldsymbol{\eta}_b}\mu_{bu,k}[t] \nabla_{\boldsymbol{\eta}_b}\mu_{bu,k}^{\mathrm{H}}[t] \;\, dt\right\}$. The non-zero elements in the FIM are presented next. Considering the b^{th} LEO satellite, the FIM focusing on the delays at the u^{th} receive antenna during the k^{th} time slot is $\boldsymbol{F}_{\boldsymbol{y}}(\boldsymbol{y}|\boldsymbol{\eta};\tau_{bu,k},\tau_{bu,k}) = -\boldsymbol{F}_{\boldsymbol{y}}(\boldsymbol{y}|\boldsymbol{\eta};\tau_{bu,k},\delta_b) = \underset{bu,k}{\mathrm{SNR}}\,\omega_{b,k}$. where $\omega_{b,k} = \left[\alpha_{1b,k}^2 + 2f_{ob,k}\alpha_{1b,k}\alpha_{2b,k} + f_{ob,k}^2\right]$.

The FIM focusing on the Doppler observed with respect to the b^{th} LEO satellite at the receiver during the k^{th} time slot is presented next. The FIM of the Doppler observed with respect to the b^{th} LEO satellite at the receiver during the k^{th} time slot is $\boldsymbol{F}_{\boldsymbol{y}}(\boldsymbol{y}|\boldsymbol{\eta};\nu_{b,k},\nu_{b,k}) = 0.5 * \underset{bu,k}{\mathrm{SNR}} f_c^2 t_{obu,k}^2$. The FIM of the Doppler observed with respect to the b^{th} LEO satellite and

[1] With the assumption that the parameters from different LEO satellites are independent.

the corresponding frequency offset during the k^{th} time slot is $\boldsymbol{F}_{\boldsymbol{y}}(\boldsymbol{y}|\boldsymbol{\eta};\nu_{b,k},\epsilon_b) = -0.5 * \underset{bu,k}{\text{SNR}} f_c t_{obu,k}^2$.

The FIM of the channel gain in the FIM due to the observations of the received signals from b^{th} LEO satellite to the u^{th} receive antenna during the k^{th} time slot is $\boldsymbol{F}_{\boldsymbol{y}}(\boldsymbol{y}|\boldsymbol{\eta};\beta_{bu,k},\beta_{bu,k}) = \frac{1}{4\pi^2|\beta_{bu,k}|^2}\underset{bu,k}{\text{SNR}}$.

The FIM focusing on the time offset at the u^{th} receive antenna during the k^{th} time slot with respect to the b^{th} LEO satellite is presented next. The FIM of the time offset in the FIM due to the observations of the received signals from b^{th} LEO satellite to the u^{th} receive antenna during the k^{th} time slot is

$$\boldsymbol{F}_{\boldsymbol{y}}(\boldsymbol{y}|\boldsymbol{\eta};\delta_b,\delta_b) = \boldsymbol{F}_{\boldsymbol{y}}(\boldsymbol{y}|\boldsymbol{\eta};\tau_{bu,k},\tau_{bu,k}) = -\boldsymbol{F}_{\boldsymbol{y}}(\boldsymbol{y}|\boldsymbol{\eta};\delta_b,\tau_{bu,k}).$$

The FIM focusing on the frequency offset at the u^{th} receive antenna during the k^{th} time slot with respect to the b^{th} LEO satellite is presented next. The FIM of the frequency offset in the FIM due to the observations of the received signals from b^{th} LEO satellite to the u^{th} receive antenna during the k^{th} time slot is $\boldsymbol{F}_{\boldsymbol{y}}(\boldsymbol{y}|\boldsymbol{\eta};\epsilon_b,\epsilon_b) = 0.5 * \underset{bu,k}{\text{SNR}} t_{obu,k}^2$.

The FIM of the channel parameters, based on the observations of the received signals, is used to derive the FIM of the receiver's location in the next section.

IV. Fisher Information Matrix for Location Parameters

In the previous section, we highlighted the useful and nuisance parameters present in the signals received from the N_B LEO satellites across the N_U receive antennas during N_K different time slots. Subsequently, we derived the information about these parameters present in the received signals and presented the structure of these parameters. In this section, we use the FIM for channel parameters to derive the FIM for the location parameters and highlight the FIM structure. This FIM for the location parameters will help us determine how feasible it is to localize a receiver with the signals received from LEO satellites.

To proceed, we define $\boldsymbol{p}_U = \boldsymbol{p}_{U,0}$ and $\boldsymbol{v}_U = \boldsymbol{v}_{U,k}$, and the location parameters $\boldsymbol{\kappa} = [\boldsymbol{p}_U, \boldsymbol{\Phi}_U, \boldsymbol{v}_U, \boldsymbol{\zeta}_1, \boldsymbol{\zeta}_2, \cdots, \boldsymbol{\zeta}_{N_B}]$, where $\boldsymbol{\zeta}_b = \left[\boldsymbol{\beta}_b^{\text{T}}, \delta_b, \epsilon_b\right]^{\text{T}}$, and our goal is to derive the FIM of the entire location parameter vector, or different combinations of parameters, under different levels of uncertainty about the channel parameters. The FIM for the location parameters, $\mathbf{J}_{\boldsymbol{y}|\boldsymbol{\kappa}}$ can be obtained from the FIM for the channel parameters, $\mathbf{J}_{\boldsymbol{y}|\boldsymbol{\eta}}$, using the bijective transformation $\mathbf{J}_{\boldsymbol{y}|\boldsymbol{\kappa}} \triangleq \boldsymbol{\Upsilon}_{\boldsymbol{\kappa}}\mathbf{J}_{\boldsymbol{y}|\boldsymbol{\eta}}\boldsymbol{\Upsilon}_{\boldsymbol{\kappa}}^{\text{T}}$, where $\boldsymbol{\Upsilon}_{\boldsymbol{\kappa}}$ represents derivatives of the non-linear relationship between the geometric channel parameters, $\boldsymbol{\eta}$, and the location parameters [11]. The elements in the bijective transformation matrix $\boldsymbol{\Upsilon}_{\boldsymbol{\kappa}}$ are given in Appendix A. With no *a priori* information about the location parameters $\boldsymbol{\kappa}$, $\mathbf{J}_{\boldsymbol{y};\boldsymbol{\kappa}} = \mathbf{J}_{\boldsymbol{y}|\boldsymbol{\kappa}}$. The EFIM taking $\boldsymbol{\kappa}_1 = [\boldsymbol{p}_U, \boldsymbol{\Phi}_U, \boldsymbol{v}_U]$ as the parameter of interest and $\boldsymbol{\kappa}_2 = [\boldsymbol{\zeta}_1, \boldsymbol{\zeta}_2, \cdots, \boldsymbol{\zeta}_{N_B}]$ as the nuisance parameters is now derived.

A. Elements in $\mathbf{J}_{\boldsymbol{y};\boldsymbol{\kappa}_1}$

The elements in $\mathbf{J}_{\boldsymbol{y};\boldsymbol{\kappa}_1}$ are presented through the following Lemmas. This FIM corresponds to the available information of the location parameters $\boldsymbol{\kappa}_1$ when the nuisance parameters are known.

Lemma 1. *The FIM of the 3D position of the receiver is*

$$\boldsymbol{F}_y(\boldsymbol{y}|\boldsymbol{\eta};\boldsymbol{p}_U,\boldsymbol{p}_U) = \sum_{b,k,u}\underset{bu,k}{\text{SNR}}\left[\frac{\omega_{b,k}}{c^2}\boldsymbol{\Delta}_{bu,k}\boldsymbol{\Delta}_{bu,k}^{\text{T}} + \frac{f_c^2 t_{obu,k}^2 \nabla_{\boldsymbol{p}_U}\nu_{b,k}\nabla_{\boldsymbol{p}_U}^{\text{T}}\nu_{b,k}}{2}\right]. \tag{3}$$

Proof. See Appendix B. □

Lemma 2. *The FIM relating the 3D position and 3D orientation of the receiver is*

$$\boldsymbol{F}_y(\boldsymbol{y}|\boldsymbol{\eta};\boldsymbol{p}_U,\boldsymbol{\Phi}_U) = \sum_{b,k,u}\underset{bu,k}{\text{SNR}}\left[\frac{\omega_{b,k}}{c}\boldsymbol{\Delta}_{bu,k}\nabla_{\boldsymbol{\Phi}_U}^{\text{T}}\tau_{bu,k}\right]. \tag{4}$$

Proof. See Appendix B. □

Lemma 3. *The FIM relating the 3D position and 3D velocity of the receiver is*

$$\boldsymbol{F}_y(\boldsymbol{y}|\boldsymbol{\eta};\boldsymbol{p}_U,\boldsymbol{v}_U) = \sum_{b,k,u}\underset{bu,k}{\text{SNR}}\left[\frac{(k-1)\omega_{b,k}\Delta_t}{c^2}\boldsymbol{\Delta}_{bu,k}\boldsymbol{\Delta}_{bu,k}^{\text{T}} - \frac{f_c^2 t_{obu,k}^2 \nabla_{\boldsymbol{p}_U}\nu_{b,k}\boldsymbol{\Delta}_{bU,k}^{\text{T}}}{2c}\right]. \tag{5}$$

Proof. See Appendix B. □

Lemma 4. *The FIM of the 3D orientation of the receiver is*

$$\boldsymbol{F}_y(\boldsymbol{y}|\boldsymbol{\eta};\boldsymbol{\Phi}_U,\boldsymbol{\Phi}_U) = \sum_{b,k,u}\underset{bu,k}{\text{SNR}}\left[\omega_{b,k}\nabla_{\boldsymbol{\Phi}_U}\tau_{bu,k}\nabla_{\boldsymbol{\Phi}_U}^{\text{T}}\tau_{bu,k}\right]. \tag{6}$$

Proof. See Appendix B. □

Lemma 5. *The FIM relating the 3D orientation and 3D velocity of the receiver is*

$$\boldsymbol{F}_y(\boldsymbol{y}|\boldsymbol{\eta};\boldsymbol{\Phi}_U,\boldsymbol{v}_U) = \sum_{b,k,u}\underset{bu,k}{\text{SNR}}\left[\frac{(k-1)\Delta_t\omega_{b,k}}{c}\nabla_{\boldsymbol{\Phi}_U}\tau_{bu,k}\boldsymbol{\Delta}_{bu,k}^{\text{T}}\right]. \tag{7}$$

Proof. See Appendix B. □

Lemma 6. *The FIM of the 3D velocity of the receiver is*

$$\boldsymbol{F}_y(\boldsymbol{y}|\boldsymbol{\eta};\boldsymbol{v}_U,\boldsymbol{v}_U) = \sum_{b,k,u}\underset{bu,k}{\text{SNR}}\left[\frac{(k-1)^2\Delta_t^2\omega_{b,k}}{c^2}\boldsymbol{\Delta}_{bu,k}\boldsymbol{\Delta}_{bu,k}^{\text{T}} + \frac{f_c^2 t_{obu,k}^2\boldsymbol{\Delta}_{bU,k}\boldsymbol{\Delta}_{bU,k}^{\text{T}}}{2c^2}\right]. \tag{8}$$

Proof. See Appendix B. □

Remark 1. *When all other location parameters are known, the information available at the k^{th} time slot for the estimation of 3D velocity through the delay is a factor $\frac{(k-1)^2\Delta_t^2}{c^2}$ more than the information available for the estimation of 3D position.*

Remark 2. *It is impossible to estimate the 3D velocity of the receiver using only the delays observed at one-time slot.*

$$
\begin{aligned}
\mathbf{J}^{\mathrm{e}}_{\boldsymbol{y};\boldsymbol{p}_U} &= [\mathbf{J}^{\mathrm{e}}_{\boldsymbol{y};\boldsymbol{\kappa}_1}]_{[1:3,1:3]} = \boldsymbol{F}_y(\boldsymbol{y}|\boldsymbol{\eta};\boldsymbol{p}_U,\boldsymbol{p}_U) - \boldsymbol{G}_y(\boldsymbol{y}|\boldsymbol{\eta};\boldsymbol{p}_U,\boldsymbol{p}_U) \\
&= \sum_{b,k,u} \underset{bu,k}{\mathrm{SNR}} \left[\frac{\omega_{b,k}}{c^2} \boldsymbol{\Delta}_{bu,k}\boldsymbol{\Delta}^{\mathrm{T}}_{bu,k} + \frac{f_c^2 t^2_{obu,k} \nabla_{\boldsymbol{p}_U}\nu_{b,k}\nabla^{\mathrm{T}}_{\boldsymbol{p}_U}\nu_{b,k}}{2} \right] \\
&- \left[\sum_b \frac{1}{c^2} \left\| \sum_{k,u} \underset{bu,k}{\mathrm{SNR}} \boldsymbol{\Delta}^{\mathrm{T}}_{bu,k}\omega_{b,k} \right\|^2 \left(\sum_{u,k} \underset{bu,k}{\mathrm{SNR}}\omega_{b,k} \right)^{-1} + \sum_b \left\| \sum_{k,u} \underset{bu,k}{\mathrm{SNR}}\ \nabla^{\mathrm{T}}_{\boldsymbol{p}_U}\nu_{b,k} \frac{(f_c)(t^2_{obu,k})}{2} \right\|^2 \left(\sum_{u,k} \frac{\underset{bu,k}{\mathrm{SNR}} t^2_{obu,k}}{2} \right)^{-1} \right].
\end{aligned} \tag{9}
$$

$$
\begin{aligned}
\mathbf{J}^{\mathrm{e}}_{\boldsymbol{y};\boldsymbol{\Phi}_U} &= [\mathbf{J}^{\mathrm{e}}_{\boldsymbol{y};\boldsymbol{\kappa}_1}]_{[4:6,4:6]} = \boldsymbol{F}_y(\boldsymbol{y}|\boldsymbol{\eta};\boldsymbol{\Phi}_U,\boldsymbol{\Phi}_U) - \boldsymbol{G}_y(\boldsymbol{y}|\boldsymbol{\eta};\boldsymbol{\Phi}_U,\boldsymbol{\Phi}_U) \\
&= \sum_{b,k,u} \underset{bu,k}{\mathrm{SNR}} \left[\omega_{b,k}\nabla_{\boldsymbol{\Phi}_U}\tau_{bu,k}\nabla^{\mathrm{T}}_{\boldsymbol{\Phi}_U}\tau_{bu,k} \right] - \sum_b \sum_{k,u\,k',u'} \underset{bu,k}{\mathrm{SNR}}\,\underset{bu',k'}{\mathrm{SNR}} \nabla_{\boldsymbol{\Phi}_U}\tau_{bu,k}\nabla^{\mathrm{T}}_{\boldsymbol{\Phi}_U}\tau_{bu',k'}\omega_{b,k}\omega_{b,k'} \left(\sum_{u,k} \underset{bu,k}{\mathrm{SNR}}\omega_{b,k} \right)^{-1}.
\end{aligned} \tag{10}
$$

$$
\begin{aligned}
\mathbf{J}^{\mathrm{e}}_{\boldsymbol{y};\boldsymbol{v}_U} &= [\mathbf{J}^{\mathrm{e}}_{\boldsymbol{y};\boldsymbol{\kappa}_1}]_{[7:9,7:9]} = \boldsymbol{F}_y(\boldsymbol{y}|\boldsymbol{\eta};\boldsymbol{v}_U,\boldsymbol{v}_U) - \boldsymbol{G}_y(\boldsymbol{y}|\boldsymbol{\eta};\boldsymbol{v}_U,\boldsymbol{v}_U) \\
&= \sum_{b,k,u} \underset{bu,k}{\mathrm{SNR}} \left[\frac{(k-1)^2\Delta_t^2\omega_{b,k}}{c^2} \boldsymbol{\Delta}_{bu,k}\boldsymbol{\Delta}^{\mathrm{T}}_{bu,k} + \frac{f_c^2 t^2_{obu,k}\boldsymbol{\Delta}_{bU,k}\boldsymbol{\Delta}^{\mathrm{T}}_{bU,k}}{2} \right] \\
&- \left[\frac{\Delta_t^2}{c^2} \sum_b \left\| \sum_{k,u} \underset{bu,k}{\mathrm{SNR}}(k-1)\boldsymbol{\Delta}^{\mathrm{T}}_{bu,k}\omega_{b,k} \right\|^2 \left(\sum_{u,k} \underset{bu,k}{\mathrm{SNR}}\omega_{b,k} \right)^{-1} + \sum_b \left\| \sum_{k,u} \underset{bu,k}{\mathrm{SNR}}\ \boldsymbol{\Delta}^{\mathrm{T}}_{bU,k} \frac{(f_c)(t^2_{obu,k})}{2c} \right\|^2 \left(\sum_{u,k} \frac{\underset{bu,k}{\mathrm{SNR}} t^2_{obu,k}}{2} \right)^{-1} \right].
\end{aligned} \tag{11}
$$

B. Elements in $\mathbf{J}^{nu}_{\boldsymbol{y};\boldsymbol{\kappa}_1}$

The elements in $\mathbf{J}^{nu}_{\boldsymbol{y};\boldsymbol{\kappa}_1}$ are presented in [1]. These elements represent the loss of information about $\boldsymbol{\kappa}_1$ due to uncertainty in the nuisance parameters $\boldsymbol{\kappa}_2$. The elements in the EFIM for the location parameters, $\mathbf{J}^{\mathrm{e}}_{\boldsymbol{y};\boldsymbol{\kappa}_1}$ are obtained by appropriately combining the Lemmas in Section IV-A and the Lemmas in Section IV-B. The EFIM for the location parameters is

$$
\mathbf{J}^{\mathrm{e}}_{\boldsymbol{y};\boldsymbol{\kappa}_1} = \mathbf{J}_{\boldsymbol{y};\boldsymbol{\kappa}_1} - \mathbf{J}^{nu}_{\boldsymbol{y};\boldsymbol{\kappa}_1} = \mathbf{J}_{\boldsymbol{y};\boldsymbol{\kappa}_1} - \mathbf{J}_{\boldsymbol{y};\boldsymbol{\kappa}_1,\boldsymbol{\kappa}_2}\mathbf{J}^{-1}_{\boldsymbol{y};\boldsymbol{\kappa}_2}\mathbf{J}^{\mathrm{T}}_{\boldsymbol{y};\boldsymbol{\kappa}_1,\boldsymbol{\kappa}_2}.
$$

C. FIM for 3D Localization

In this section, we consider available information for estimating one of the location parameters when the other two location parameters are known. We start with the FIM for the 3D position estimation when both the 3D orientation and 3D velocity are known, and then we proceed to the FIM for the 3D orientation estimation when both the 3D position and 3D velocity are known. Finally, we present the FIM for the 3D velocity estimation when the 3D position and 3D orientation are known.

Theorem 1. *First, when both the 3D orientation and 3D velocity are known, the EFIM of the 3D position of the receiver is given by (9). Second, when both the 3D position and 3D velocity are known, the EFIM of the 3D orientation of the receiver is given by (10). Finally, when both the 3D position and 3D orientation are known, the EFIM of the 3D velocity of the receiver is given by (11).*

Proof. The proof follows by subtracting the appropriate Lemmas in Section IV-B from the Lemmas in Section IV-A, following the EFIM definition and then selecting the appropriate diagonal. □

Next, we derive the FIM for 9D localization in terms of the FIM for 3D localization.

D. FIM for 9D Localization

In this section, we analyze the FIM when all location parameters are unknown. More specifically, we present the available information when all the location parameters - 3D position, 3D orientation and 3D velocity are parameters to be estimated.

Theorem 2. *If $\mathbf{J}^{\mathrm{e}}_{\boldsymbol{y};\boldsymbol{\Phi}_U}$ is invertible then the loss in information about $\boldsymbol{p}_U$ due to the unknown $\boldsymbol{\Phi}_U$ and $\boldsymbol{v}_U$ which is specified by $\mathbf{J}^{nu}_{\boldsymbol{y};\boldsymbol{p}_U}$ exists if and only if $\boldsymbol{S} = \mathbf{J}^{\mathrm{e}}_{\boldsymbol{y};\boldsymbol{v}_U} - \mathbf{J}^{\mathrm{e}}_{\boldsymbol{y};[\boldsymbol{v}_U,\boldsymbol{\Phi}_U]}[\mathbf{J}^{\mathrm{e}}_{\boldsymbol{y};\boldsymbol{\Phi}_U}]^{-1}\mathbf{J}^{\mathrm{e}}_{\boldsymbol{y};[\boldsymbol{\Phi}_U,\boldsymbol{v}_U]}$ is invertible. Subsequently, $\mathbf{J}^{nu}_{\boldsymbol{y};\boldsymbol{p}_U}$ is given by (13), and the EFIM for the 3D position in this 9D localization scenario is*

$$
\mathbf{J}^{\mathrm{eee}}_{\boldsymbol{y};\boldsymbol{p}_U} = \mathbf{J}^{\mathrm{e}}_{\boldsymbol{y};\boldsymbol{p}_U} - \mathbf{J}^{nu}_{\boldsymbol{y};\boldsymbol{p}_U}. \tag{12}
$$

Proof. See Appendix B. □

V. Numerical Results

This section presents simulation results that describe the available information in signals received from LEO satellites during multiple transmission time slots on receivers with multiple antennas. We start by showing the minimum infrastructure needed to estimate different location parameters. More specifically, we present the minimum number of LEO satellites, time slots, and receive antennas that contribute to 3D position, 3D velocity, and 3D orientation estimation. We also present the Cramer Rao bound (CRB) for 3D position, 3D orientation, and 3D velocity estimation in the 9D localization case. We present the CRB for the 3D position as a function of the spacing between transmission time slots.

We use the following simulation parameters. The SNR is assumed constant across the transmission time slots and receive antennas, and the following set of SNR values is considered: $\{40\ \mathrm{dB}, 20\ \mathrm{dB}, 0\ \mathrm{dB}, -20\ \mathrm{dB}\}$. The x,y, and z components of

$$
\begin{aligned}
\mathbf{J}^{nu}_{\boldsymbol{y};\boldsymbol{p}_U} = {} & \mathbf{J}^{e}_{\boldsymbol{y};[\boldsymbol{p}_U,\boldsymbol{\Phi}_U]}[\mathbf{J}^{e}_{\boldsymbol{y};\boldsymbol{\Phi}_U}]^{-1}\mathbf{J}^{e}_{\boldsymbol{y};[\boldsymbol{\Phi}_U,\boldsymbol{p}_U]} + \mathbf{J}^{e}_{\boldsymbol{y};[\boldsymbol{p}_U,\boldsymbol{\Phi}_U]}[\mathbf{J}^{e}_{\boldsymbol{y};\boldsymbol{\Phi}_U}]^{-1}\mathbf{J}^{e}_{\boldsymbol{y};[\boldsymbol{\Phi}_U,\boldsymbol{v}_U]}\boldsymbol{S}^{-1}\mathbf{J}^{e}_{\boldsymbol{y};[\boldsymbol{v}_U,\boldsymbol{\Phi}_U]}[\mathbf{J}^{e}_{\boldsymbol{y};\boldsymbol{\Phi}_U}]^{-1}\mathbf{J}^{e}_{\boldsymbol{y};[\boldsymbol{\Phi}_U,\boldsymbol{p}_U]} \\
& - \mathbf{J}^{e}_{\boldsymbol{y};[\boldsymbol{p}_U,\boldsymbol{v}_U]}\boldsymbol{S}^{-1}\mathbf{J}^{e}_{\boldsymbol{y};[\boldsymbol{v}_U,\boldsymbol{\Phi}_U]}[\mathbf{J}^{e}_{\boldsymbol{y};\boldsymbol{\Phi}_U}]^{-1}\mathbf{J}^{e}_{\boldsymbol{y};[\boldsymbol{\Phi}_U,\boldsymbol{p}_U]} - \mathbf{J}^{e}_{\boldsymbol{y};[\boldsymbol{p}_U,\boldsymbol{\Phi}_U]}[\mathbf{J}^{e}_{\boldsymbol{y};\boldsymbol{\Phi}_U}]^{-1}\mathbf{J}^{e}_{\boldsymbol{y};[\boldsymbol{\Phi}_U,\boldsymbol{v}_U]}\boldsymbol{S}^{-1}\mathbf{J}^{e}_{\boldsymbol{y};[\boldsymbol{v}_U,\boldsymbol{p}_U]} \\
& + \mathbf{J}^{e}_{\boldsymbol{y};[\boldsymbol{p}_U,\boldsymbol{v}_U]}\boldsymbol{S}^{-1}\mathbf{J}^{e}_{\boldsymbol{y};[\boldsymbol{v}_U,\boldsymbol{p}_U]}.
\end{aligned}
\tag{13}
$$

the position of the LEO satellites are randomly chosen, but LEO satellites are approximately 2000 km from the receiver. The x,y, and z components of the velocity of the LEO satellites are randomly chosen and change every transmission time slot to depict acceleration, but the LEO satellites have a speed of 8000 m/s. The receiver's position's x,y, and z components are randomly chosen, but the receiver is approximately 30 m from the origin. The x,y, and z components of the receiver's velocity are randomly chosen and remain constant to depict constant velocity, but the receiver has a speed of 25 m/s. The effective baseband bandwidth, $\alpha_{1b,k}$, is 100 MHz and the BCC, $\alpha_{2b,k}$, is 0 MHz.

A. Information available to find the 3D position of the receiver when the 3D velocity and 3D orientation are unknown

1) $N_K = 3$, $N_B = 3$, and $N_U > 1$: Even in the presence of both offsets, there is enough information to estimate: i) $\mathbf{J}^{\mathrm{e}}_{\boldsymbol{y};\boldsymbol{\Phi}_U}$, ii) $\mathbf{J}^{\mathrm{e}}_{\boldsymbol{y};\boldsymbol{v}_U}$, and iii) $\mathbf{J}^{\mathrm{ee}}_{\boldsymbol{y};\boldsymbol{v}_U}$. Hence, the loss in information about $\boldsymbol{p}_U$ due to the unknown $\boldsymbol{\Phi}_U$ and $\boldsymbol{v}_U$ which is specified by $\mathbf{J}^{nu}_{\boldsymbol{y};\boldsymbol{p}_U}$ exists. Further, since there is enough information to estimate $\mathbf{J}^{\mathrm{e}}_{\boldsymbol{y};\boldsymbol{p}_U}$ then $\mathbf{J}^{\mathrm{eee}}_{\boldsymbol{y};\boldsymbol{p}_U}$ can also be estimated by Theorem 2. Simulation results verify that there is enough information for $\mathbf{J}^{\mathrm{eee}}_{\boldsymbol{y};\boldsymbol{p}_U}$ to be positive definite. Hence, $\boldsymbol{p}_U$ can be estimated in the presence of both offsets.

2) Simulation results: Here, we present simulation results for the CRLB when estimating $\boldsymbol{p}_U$ with $N_K = 3$, $N_B = 3$, *and* $N_U > 1$. In Fig. 2, we notice an improvement in positioning error due to an increase in the length of the time interval between the transmission time slots is more clearly seen. This reduction in positioning error is slow from 25 ms to 100 ms but is drastic above 100 ms. This improvement in positioning error is due to the speed of the LEO satellites. The speed of satellites means that the same satellite can act as multiple anchors in different time slots while still achieving good geometric dilution of precision.

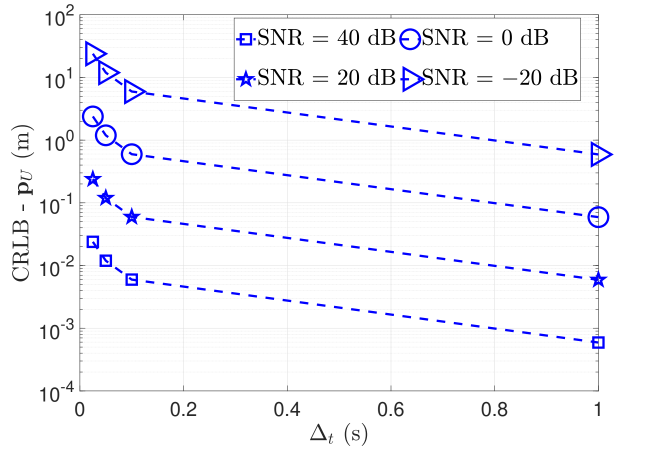

Figure 2. CRLB for $\boldsymbol{p}_U$ in the 9D localization scenario with $f_c = 1$ GHz and $N_U = 4$: focuses on Δ_t values from $\Delta_t = 25$ ms to $\Delta_t = 1$ s.

VI. Conclusion

In this paper, we have investigated the conditions that allow for the estimation of a receiver's 3D position, 3D orientation, and 3D velocity using the signals received from LEOs. We discovered that even in the presence of time and frequency offsets between the LEOs, it is possible to perform 9D localization (3D position, 3D velocity, and 3D orientation estimation) of a receiver by utilizing the signals from three LEO satellites observed during three transmission time slots received through multiple receive antennas.

Appendix

A. Entries in transformation matrix

See [1]

B. Proof of Lemmas and Theorems

See [1].

References

[1] D.-R. Emenonye, H. S. Dhillon, and R. M. Buehrer, "Fundamentals of LEO based localization," *in preparation to* IEEE Trans. on Info. Theory, 2024.

[2] M. L. Psiaki, "Navigation using carrier doppler shift from a LEO constellation: TRANSIT on steroids," *NAVIGATION*, vol. 68, no. 3, pp. 621–641, 2021. [Online]. Available: https://onlinelibrary.wiley.com/doi/abs/10.1002/navi.438

[3] Z. M. Kassas, J. Morales, and J. J. Khalife, "New-age satellite-based navigation – STAN: Simultaneous tracking and navigation with LEO satellite signals," 2019. [Online]. Available: https://api.semanticscholar.org/CorpusID:214300844

[4] J. Khalife, M. Neinavaie, and Z. M. Kassas, "Navigation with differential carrier phase measurements from megaconstellation LEO satellites," in *Proc., IEEE/ION Position, Location and Navigation Symposium (PLANS)*, 2020, pp. 1393–1404.

[5] J. Haidar-Ahmad, N. Khairallah, and Z. M. Kassas, "A hybrid analytical-machine learning approach for LEO satellite orbit prediction," in *proc., International Conference on Information Fusion (FUSION)*, 2022, pp. 1–7.

[6] M. Neinavaie, J. Khalife, and Z. M. Kassas, "Acquisition, doppler tracking, and positioning with starlink LEO satellites: First results," *IEEE Trans. on Aerospace and Electronic Systems*, vol. 58, no. 3, pp. 2606–2610, Apr. 2022.

[7] Z. M. Kassas, N. Khairallah, and S. Kozhaya, "Ad astra: Simultaneous tracking and navigation with megaconstellation LEO satellites," *IEEE Aerospace and Electronic Systems Magazine*, to appear.

[8] J. Haidar-Ahmad, N. Khairallah, and Z. M. Kassas, "A hybrid analytical-machine learning approach for LEO satellite orbit prediction," in *25th International Conference on Information Fusion (FUSION)*, 2022, pp. 1–7.

[9] S. M. LaValle, *Planning Algorithms*. Cambridge University Press, 2006.

[10] Y. Shen and M. Z. Win, "Fundamental limits of wideband localization — part I: A general framework," *IEEE Trans. on Info. Theory*, vol. 56, no. 10, pp. 4956–4980, Oct. 2010.

[11] S. M. Kay, *Fundamentals of Statistical Signal Processing: Estimation Theory*. Prentice-Hall, Inc., 1993.